MICROWAVE HOLOGRAPHY IMAGING ARRAY FOR EARLY BREAST CANCER DETECTION

Wang, L., Kitaeff, V., Al-Jumaily, A.M.
Institute of Biomedical Technologies
Auckland University of Technology, Auckland, NZ
luwang@aut.ac.nz

***Abstract*—This paper presents a new microwave holography imaging array (MHIA) technique for early breast cancer detection, which is based on a microwave holography technique. The analytical mathematical model is developed under the MATLAB environment to demonstrate the proposed imaging technique, which is able to compute the unknown tumor size and its location inside the breast model. The simulation results show that tumors as small as 1 mm in diameter anywhere within the breast can be successfully detected, even as close as 2 mm from the skin layer. The significant imaging improvement is achieved by optimizing antenna-sensor array configurations to offer the best possibility of detecting tumors of various size, shape and position, as well as increasing the number of receptors-antennas to 16. This approach offers significant benefits in terms of providing complementary, safe and better imaging in real-time at significantly lower cost.**

***Index Terms*—Microwave Imaging, Microwave Holography Imaging Array, Breast Cancer Detection, Interferometric**

I. INTRODUCTION

Breast cancer is the most frequently diagnosed cancer and the second leading cause of cancer death among females [1]. Early detection of breast cancer by regular breast screening detection with treatment has been shown to sharply reduce the breast cancer related mortality and increase the survival rate [2].

Microwave Imaging (MI) is one of the most promising complimentary to X-ray mammography techniques for early detection of breast cancer. MI has been the subject of much study for a couple of decades [3]. Unlike X-rays, which detects structural changes in tissue cells, microwaves detect changes in dielectric properties, which occur before the structural changes occur [3], which can potentially be useful for earlier detection of breast cancer.

Using electromagnetic waves of radio range for non-invasive diagnostics and imaging of human organs has been tried by many [4]-[11]. The idea has been to exploit the differences in dielectric permittivity of various human tissues creating the reflections of radio waves [7],[12]-[13]. It has been shown that malignant and healthy tissues have different dielectric properties due to the higher water content in cancerous tissue [14]. Normal breast tissue, which is mostly fatty tissue, is generally transparent for the microwaves till up to 10GHz. So far the most developed approach exploits variations of Synthetic Aperture RADAR (SAR) techniques [7]-[10].

Holographic technique has recently been reported as a potential competitor to SAR in microwave breast cancer detection [15]-[17]. In contrast with SAR, microwave holography does not require expensive ultra high speed electronics, as narrow-band signal is used enabling real-time imaging at significantly lower cost [18]. Another advantage is that holographic can be made insensitive to the reflections from the skin and chest wall by limiting the resolution to the objects of a size close to the expected cancerous structures in breast $e.g.$ 1-30 mm.

In this paper, Microwave Holography Imaging Array (MHIA) for early breast cancer detection is described based on real-time aperture synthesis imaging technique similar to the one widely used in radio astronomy. The analytical mathematical foundation of the method and computer simulations for selected array configurations are presented. The rest of the paper is organized as follows. Section II describes in detail the theory of the proposed MHIA technique. Section III explains the proposed imaging system and Section IV discusses the array configuration. Simulation results are presented in Section V. Finally, some conclusions are drawn in Section VI.

II. THEORY

Cancerous tumors are radio passive and in MHIA they are illuminated with continuous nearly monochromic radio wave. A contrast in permittivities of cancerous and healthy tissues causes some of the power of microwaves to be scattered back. This backscattered radiation can be then received by an array of microwave receptors-antennas and analyzed.

The imaging setup generally is thought to look as presented of Fig. 1. The patient lies face-down on the table in prone position with her breast flattered against the table. The table has a window against patient breasts made of material with dielectric properties close to the normal average breast tissue. The receptor array is placed at some distance away from the patient with one of the elements being a transmitter and others receivers. The space between the table and array is filled with the same material the table window. In order to prevent an unwanted interferences from the outside the system is concealed in a microwave absorbent material cylinder.

Lets consider a pair of receptors in the array forming a two-element interferometer (see Fig. 2a). The receptors A_1 and A_2 are separated at a distance D, baseline, seeing the same tumor in the far field of interferometer. The backscattered signal R_1 from a tumor reaches A_1 at a geometrical time delay τ before the backscattered signal R_2 reaches A_2, the fringe function of such interferometer is

$$F(\tau) = 2sin(2\pi vt)sin2\pi v(t-\tau) \quad (1)$$

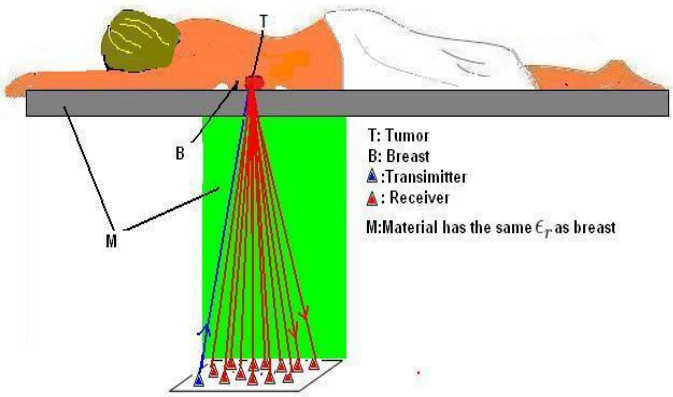

Fig. 1: MHIA system

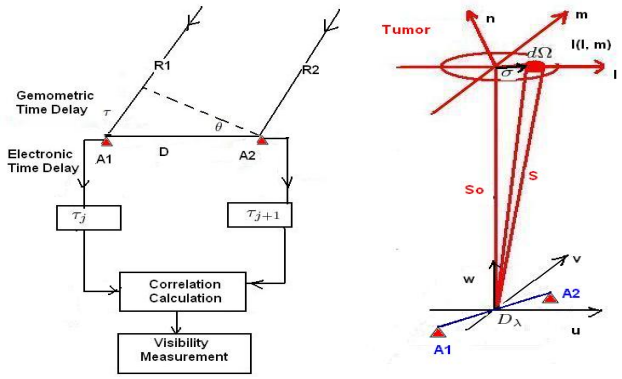

(a) (b)

Fig. 2: Measurement setting (a) The visibility is the measurement of spatial correlation between the electric field of receptor pairs (b) A distant tumor is observed by an receptor pair. The baseline connecting the two receptors is the origin of the (u, u, w) coordinate system. The w axis points from the baseline toward the reference direction s_o of tumor

Where t is time, v is frequency. Considering the far field case $R_1, R_2 \gg D$, and the geometrical time difference τ in signal arrival to two different receptors can be calculated as

$$\tau = \frac{D}{c} sin(\theta) \tag{2}$$

c is the velocity of light that less by factor $\sqrt{\epsilon_r}$ (the relative dielectric permittivity ϵ_r is 9 for breast tissue). Thus Eq. 1 can be rewritten as

$$F_I(\theta) = 2sin(2\pi vt) sin 2\pi v(t - \frac{D\sqrt{\epsilon_r}}{c} sin(\theta)) \tag{3}$$

For a coherently multiplied array of N receptors the total fringe pattern is:

$$F_T = B \sum_{1}^{M} F/N \tag{4}$$

Where $M = \frac{N(N-1)}{2}$ is the number of unique baselines for each pair of receptors in the array, and B is a receptor beam function.

The output of such an interferometer is a convolution of the fringe pattern F_T and the tumor brightness function A:

$$V = \int F_T(\sigma) A(\sigma) e^{-j2\pi D_\lambda \bullet \sigma} d\Omega, \tag{5}$$

Where $D_\lambda = \frac{D}{\lambda}$ is the baseline in wavelength, $d\Omega$ is the solid angle at position s=s_o+σ (see Fig. 2b).

Eq. 5 can be rewritten in a rectangular coordinate system as shown in Fig. 2b. The vector σ is then can be denoted as:

$$\sigma = (l, m, \sqrt{1 - l^2 - m^2} - 1) \tag{6}$$

The solid angle $d\Omega$ is then as:

$$d\Omega = \frac{dldm}{\sqrt{1 - l^2 - m^2}} \tag{7}$$

Let also the coordinates of the array be given in a rectilinear coordinate system (u, v, w). Eq. 5 then becomes as:

$$V(u, v) = \int_{-\infty}^{\infty} \int_{-\infty}^{\infty} \frac{F_T(l, m) A(l, m)}{\sqrt{1 - l^2 - m^2}} e^{-j2\pi(ul+vm)} dldm \tag{8}$$

For a tumor with visibility measurements covering the entire (u, v) domain, the tumor image is perfectly computed by the Fourier inversion of the visibility. The (u, v) domain can be measured by sampling the receptor pair baselines in the array, which is known as the (u, u) coverage [19]. This coverage is determined by many factors with array configuration as the most important one.

Let $S(u, v)$ be the sampling function ($S(u, v)$=1 for each measured (u, v) pair and otherwise $S(u, v)$=0). The image is then obtained by:

$$Image(l, m) = \int \int V(u, v) S(u, v) e^{j2\pi(ul+vm)} dudv \tag{9}$$

The synthesized beam $B(l, m)$ is defined as:

$$B(l, m) = \int \int S(u, v) e^{j2\pi(ul+vm)} dudv \tag{10}$$

Now, the image becomes the convolution of the tumor brightness distribution $I(l, m)$ and the synthesized beam $B(l, m)$:

$$Image(l, m) = I(l, m) * B(l, m) \tag{11}$$

Where $I(l, m) = F_T(l, m) A(l, m)$.

To reconstruct an image, a two-dimensional Inverse Fast Fourier Transform (IFFT) is applied:

$$g(i, k) = \sum_{p=0}^{M-1} \sum_{q=0}^{N-1} f(p, q) e^{j2\pi ip/M} e^{j2\pi kq/N} \tag{12}$$

The functions are periodic with periods of M samples in the i and p dimensions and N samples in the k and q dimensions.

III. Simulations For Various Array Configurations

The simulations presented in this paper as approximated by 3D Gaussian function having no well defined shape boundaries, which is sufficiently adequate to simulate a tumor at early development stage.

The configurations of existing arrays have been studied to produce good sampling of the visibility function, which can produce high quality breast images. The goal of most future array configuration studies is to produce (u, v) sampling with a truncated Gaussian density distribution, and thus synthesized beams with a nearly Gaussian profile. For imaging, logarithmic spiral array configurations are favored because they provide dense sampling of the aperture plane over a wide range of projected baseline lengths [20].

In this research, an array of receptors are randomly located on a flat plane that is in a spiral array configuration. MATLAB random function is employed to display the array locations in (x, y) dimensional:

$$(x, y) = rand(N, 2)L \tag{13}$$

Where N is receptor number and L is array plane length.

A logarithmic spiral random function is developed to display the (x, y) locations of each receptor on array plane is

$$x = \frac{L(tcos(t) + \min \|tcos(t)\|)}{\max \|tcos(t)\| + \min \|tcos(t)\|} \tag{14}$$

$$y = \frac{W(tsin(t) + \min \|tsin(t)\|)}{\max \|tsin(t)\| + \min \|tsin(t)\|} \tag{15}$$

Where t=linspace(aπ,π/b,N), a is anticlockwise rotation angle, b is clockwise rotation angle, N is receptor number, L is array plane length and W is array plane width.

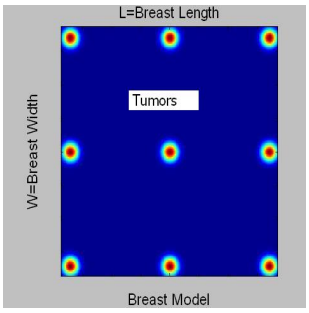

Fig. 3: 2D view of the assumed breast box with tumors in nine locations

The breast is a hemispherical model that is R mm in diameter and d mm in depth. For better breast cancer detection, breast needs to be compressed firmly. In this case, the breast model is assumed as a box ($L = R$ mm x $W = R$ mm x $D = d/2$ mm). For a clinically viable imaging system, a malignant lump can be located anywhere within a breast. Thus, tumors at nine locations within the breast have been investigated (see Fig. 3). All nine positions represent challenging cases of tumors in a close proximity of the skin layer and chest wall. Four breast models in cup size range from A to H (see Table I) with nine tumors in diameter of 1 mm, 3 mm and 30 mm are selected to simulate respectively.

TABLE I: Breast Model size [21]

Breast Model	Width (mm)	Length (mm)	Depth (mm)
A cup	120	120	120
B cup	140	140	140
C cup	160	160	160
D cup	180	180	180
H cup	≥ 270	≥ 270	≥ 270

In simulation, a 2D analytical mathematical model is developed to demonstrate the proposed MHIA technique. The performance of the simulations have been completed under MATLAB environment. More than 80 different array configurations are investigated in this study, four of them are selected and compared in this paper. 16 antennas are located in the flat array plane (100 mm x 100 mm) in array configuration under the selected 4 array configurations, which are displaying in Fig. 4. The distance between array plane and breast model is 4500 mm.

Fig. 5 and Fig. 6 display the snapshot UV coverages and reconstructed images of breast with tumor of 3 mm in diameter under the four selected array configurations. Reconstructed images of breast in Fig. 5a is obtained Eq. 13, while reconstructed images of brest in Fig. 5b and Fig. 5c are obtained with using the developed array configuration algorithms (see Eq. 14 & Eq. 15).

It is can be seen that the spatial frequency coverage in Fig. 5b is more satisfactory than others in Fig. 5, which is able to generate a real image of breast. Fig. 6b shows tumors of size, shape and location can be successfully detected and displayed under array configuration (b). Fig. 6 shows the original and reconstructed images of breast (A cup) with tumors under the selected four array configurations $(a)-(d)$, it is can be seen that the reconstructed breast image displays the most clearly and accurate tumor informations is under array configuration (b) (see Fig. 6d).

In order to test the proposed technique provides reliable imaging apparatus, breasts with different size and tumors with different size and locations (see Fig. 3) are simulated under array configuration (b). Fig. 7 shows the original and reconstructed images of breasts (A-D cup in size) with tumors of 1 mm in diameter. While, Fig. 8 shows the original and reconstructed images of breasts (A-D cup in size) with tumors of 3 mm in diameter. Fig. 9 shows the original and reconstructed images of breast (H cup in size) with tumors of 5 mm and 10mm in diameter respectively.

Compare the reconstructed images and the original images of breasts in Fig. 7 - Fig. 9, the simulation results show that all tested tumors in different size and locations are successfully detected and clearly identified in the reconstructed breast images.

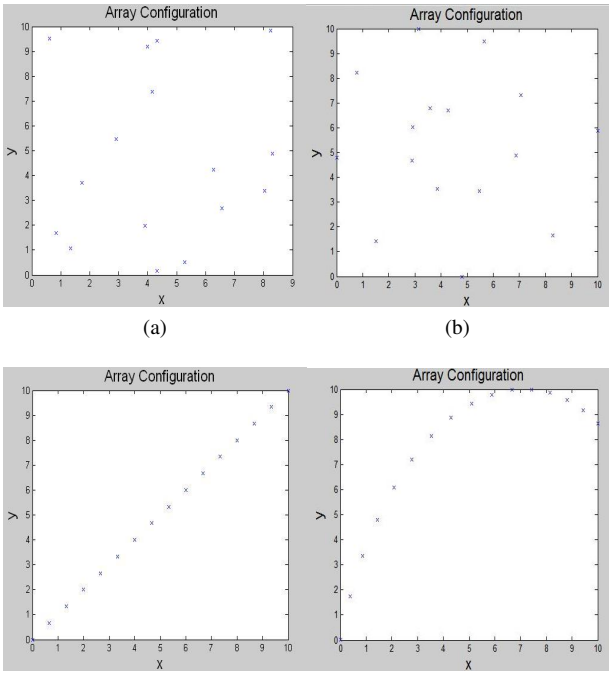

(a) (b)

(c) (d)

Fig. 4: Array configurations

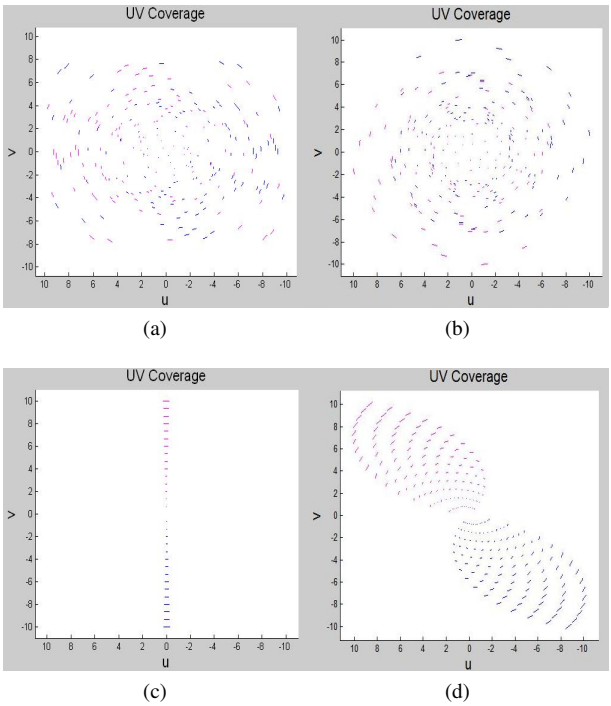

(a) (b)

(c) (d)

Fig. 5: Snapshot of UV Coverages with array configurations

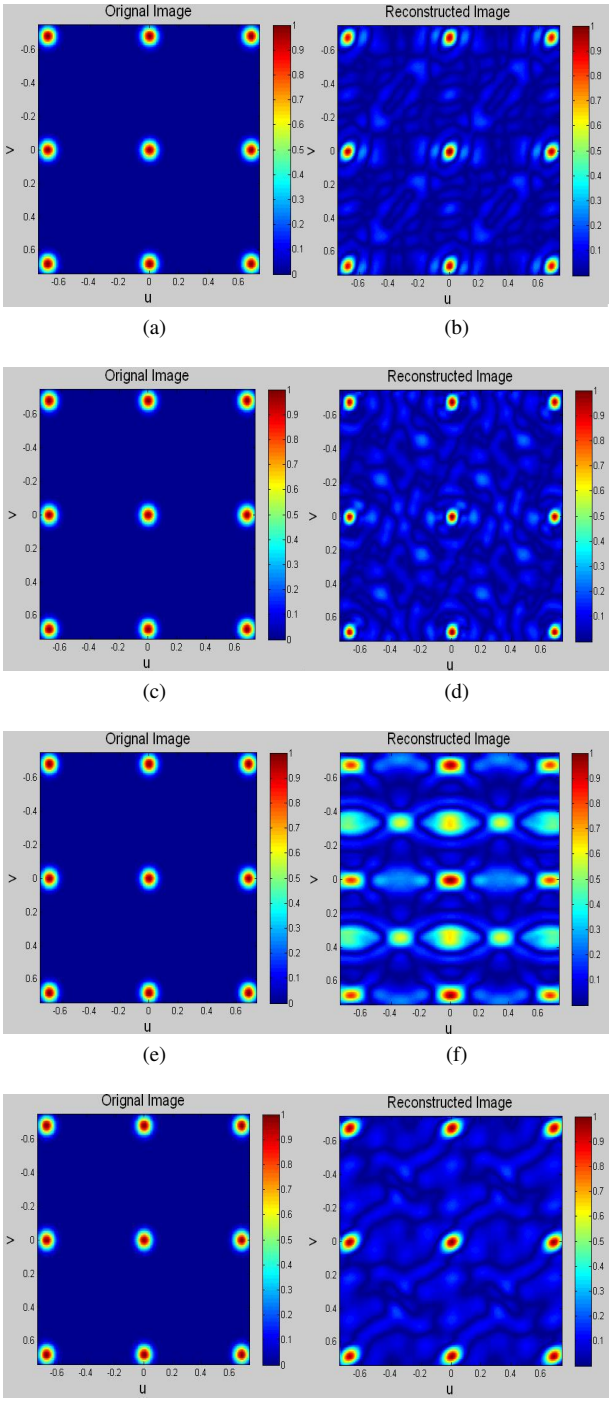

(a) (b)

(c) (d)

(e) (f)

(g) (h)

Fig. 6: Original (left column) and Reconstructed (right column) Images of A cup breast with tumor of 3 mm in diameter under array configurations

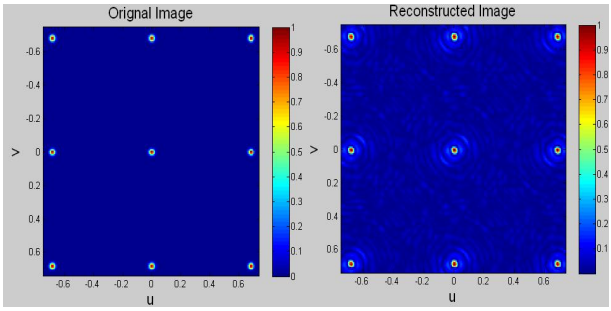

(a) (b)

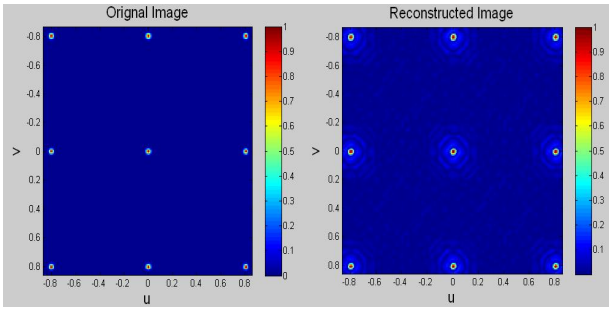

(c) (d)

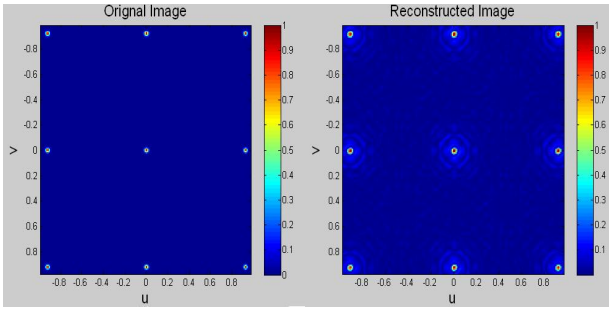

(e) (f)

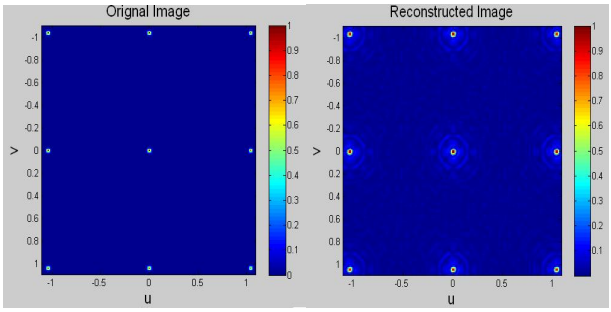

(g) (h)

Fig. 7: Original (left column) and Reconstructed (right column) image with tumor of 1 mm in diameter in (a-b) A cup breast (c-d) B cup breast (e-f) C cup breast (g-h) D cup breast

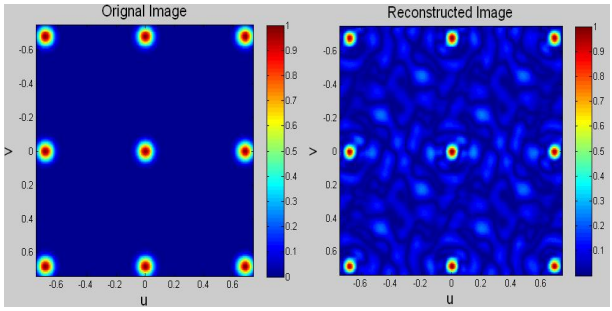

(a) a (b) b

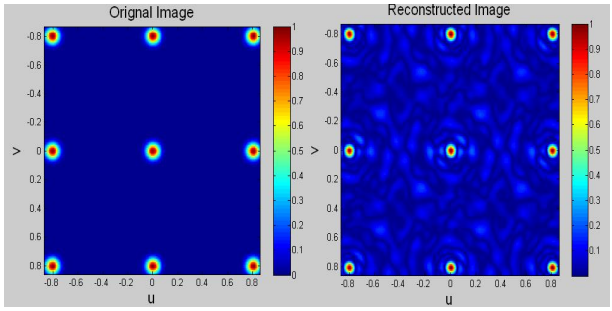

(c) c (d) d

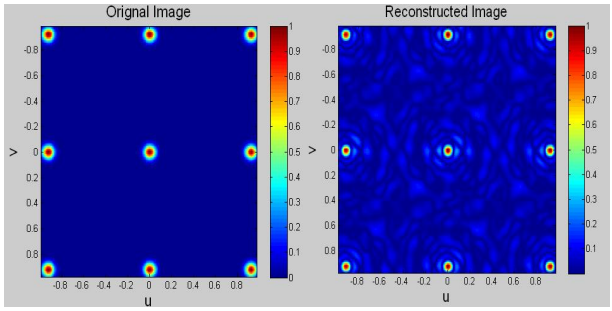

(e) e (f) f

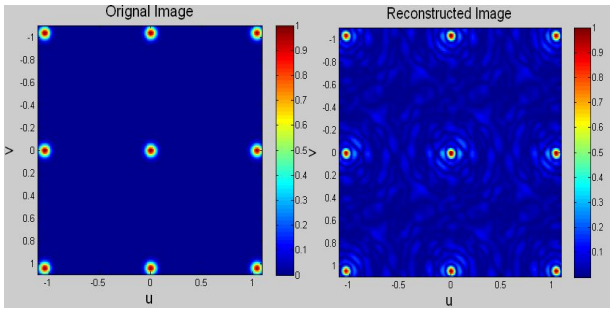

(g) g (h) h

Fig. 8: Original (left column) and Reconstructed (right column) image with tumor of 3 mm in diameter in (a-b) A cup breast (c-d) B cup breast (e-f) C cup breast (g-h) D cup breast

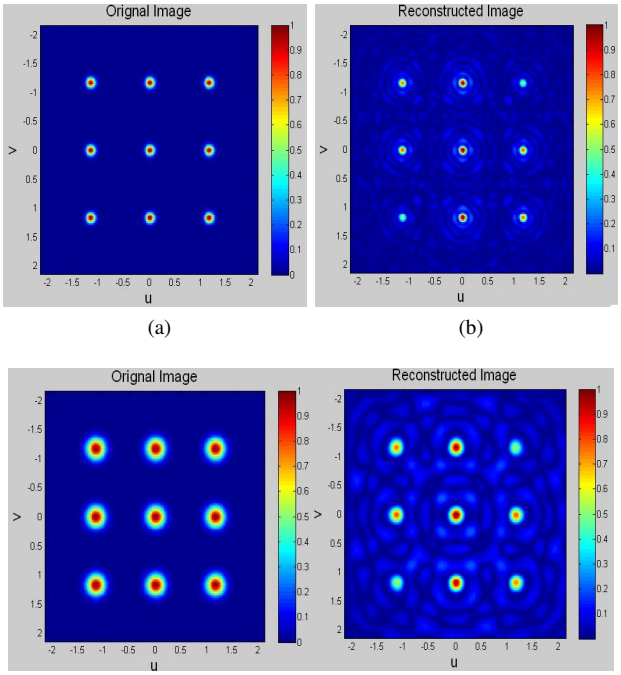

(a) (b)

(c) (d)

Fig. 9: Original (left column) and Reconstructed (right column) image of H cup breast with tumor of (a-b) 5 mm in diameter (c-d) 5 mm in diameter

IV. Conclusions

In this paper, a new improved microwave holography imaging array for early beast cancer detection is introduced, which is based on real-time aperture synthesis imaging technique. The significant imaging improvement of the 16-element array has been demonstrated. One of the key reasons to obtaining excellent result is the optimization of array configurations.

The best array configuration (b) has been achieved, tumors in different size (1 mm, 3 mm, 5 mm and 10 mm in diameter) within anywhere of breasts (A to H cup in size) are simulated under the best array configuration (b). The simulation results show that all tested tumors successfully obtained (see Fig. 7 - Fig. 9).

To summary, the proposed MHIA technique is able to detect very small tumor (1 mm in diameter) in any location within the breast, even as close as 2 mm from the chest wall. It is able to presents the correct information of tumor size, shape and location. Comparing to previous researches, this approach offers significant benefits in terms of providing complementary, safe and better real-time imaging at significantly lower cost.

References

[1] Liu G.D. and Zhang Y.R., *An Overview of Active Microwave Imaging for Early Breast Cancer Detection*. Journal of Nanjing University of Posts and Telecommunications (Natural Science), 30 (1), 2010.

[2] Smith R.A., Saslow D., Sawyer K.A., Burke W., Costanza M.E., Evans W.P., Foster R.S., Hendrick H.J.E.E. and Sener S., *American cancer society guidelines for breast cancer screening: Updated 2003*. CA: A Cancer J for Clinician, 2003.

[3] Lee A., *Types of Medical Imaging: X-ray, Ultrasound, Magnetic, and Nuclear Modalities*. Available : http://www.suite101.com/content/typesof-medicalimaginga85622#ixzz1GX1hQUQL, Dec 20, 2008.

[4] X. Zhuge, M. Hajian, A.G. Yarovoy, L.P. Ligthart *Ultra-Wideband Imaging for Detection of Early-Stage Breast Cancer*. Proceedings of the 4th European Radar Conference, pp.39 - 42, October, 2007.

[5] Elsdon M., Leach M., FDO M.J., Foti S.J. and Smith D., *Early Stage Breast Cancer Detection using Indirect Microwave Holography*. Microwave Conference, 2006. 36th European, pp.1256 - 1259, 10-15 Sept, 2006.

[6] Carr K.L., Cevasco P., Dunlea P. and Shaeffer, J., *Radiometric sensing: an adjuvant to mammography to determine breast biopsy* . IEEE MTT-S International Microwave Symposium Digest, 2 (2) : pp.929-932, 06 August, 2002.

[7] Fear E. C., Li X., Hagness S. C. and Stuchly M. A., *Confocal microwave imaging for breast cancer detection: Localization of tumors in three dimensions*. IEEE Transactions on Biomedical Engineering, 49 (8) : pp.812-822, 2002.

[8] Bond E. J., Li, X., Hagness S. C. and Van Veen B. D., *Microwave imaging via space-time beamforming for early detection of breast cancer*. IEEE Transactions on Antennas and Propagation, 51 (8) : pp.1690-1705, 2003.

[9] Sill J. M. and Fear E. C., *Tissue sensing adaptive radar for breast cancer detection - experimental investigation of simple tumor models*. IEEE Transactions on Microwave Theory and Techniques, 53 (11) : pp.3312 - 3319, Nov, 2005.

[10] Davis S. K., Tandradinata H., Hagness S. C. and Van Veen B. D., *Ultrawideband microwave breast cancer detection: a detection-theoretic approach using the generalized likelihood ratio test*. IEEE Transactions on Biomedical Engineering, 52 (7) : pp.1237-125053, 2005.

[11] Smith D., Leach M., Elsdon M. and Foti S. J., *Indirect Holographic Techniques for Determining Antenna Radiation Characteristics and Imaging Aperture Fields* . IEEE Transactions on Antennas and Propagation Magazine, 49 (1) : pp.54 - 67, 11 June, 2007.

[12] Gabriel C. and Peyman A. *Dielectric measurement: Error analysis and assessment of uncertainty*. Physics in Medicine and Biology, 51 (23) : pp.6033-6046, 2006.

[13] Gabriel S., Lau R. W. and Gabriel C *The dielectric properties of biological tissues: II. Measurements in the frequency range 10 Hz to 20 GHz*. Physics in Medicine and Biology, 41 (11) : pp.2251-2269, 1996(a).

[14] Yuanwei J., Yi J. and Moura J. *Time Reversal Beamforming for Microwave Breast Cancer Detection*. IEEE International Conference on Image Processing, 2007, 5 : pp. 13-16, November 12, 2007.

[15] Michael E., Sergei Skobelev M.L. and Smith D., *Microwave Holographic Imaging of Breast Cancer*. Microwave, Antenna, Propagation and EMC Technologies for Wireless Communications,International Symposium on 2007, pp. 966 - 969, 2007.

[16] Sudhir Shrestha, M.A., Joshua Reid and Kody Varahramyan, *Microstrip Antennas for Direct Human Skin Placement for Biomedical Applications*. PIERS Proceedings, Cambridge, USA, July 5-8, 2010.

[17] Shakti K. Davis, B.D.V.V., Susan C. Hagness and Frederick K., *Breast Tumor Characterization Based on Ultrawideband Microwave Backscatter*. IEEE TRANSACTIONS ON BIOMEDICAL ENGINEERING, 55 (1), 2008.

[18] Smith D., M.L., Michael E. and Fbti S.J., *Indirect Holographic Techniques for Determining Antenna Radiation Characteristics and Imaging Aperture Fields*. IEEE TRANSACTIONS ON ANTENNAS AND PROPAGATION, 2007.

[19] Levanda R. and Leshem A., *Synthetic aperture radio telescopes* . IEEE Signal Processing Magazine, 27 (1) : pp. 14 - 29, Jan, 2010.

[20] Jones D.L., *Geometric Configurations for Large Spacecraft-Tracking Arrays*. IEEE, 2 : pp. 2-997, 2003.

[21] Sizing Guide, *Available*: http://www.lingerie-bodyfashion.com/maten.asp?lang=en, August 15, 2011.